H. 713

OCTOBER 1978 PPPL-1484

UC-20f

CONF-780662--2

PLT NEUTRAL INJECTOR PERFORMANCE

PLASMA PHYSICS LABORATORY

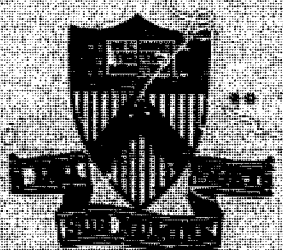

PRINCETON UNIVERSITY
PRINCETON, NEW JERSEY

PLT NEUTRAL INJECTOR PERFORMANCE

L. R. Grisham, H. P. Eubank, H. F. Dylla, R. J. Goldston,
G. Schilling, L. D. Stewart*, R. W. Stookesberry†, M. Ulrickson

Plasma Physics Laboratory, Princeton University
Princeton, New Jersey 08540

PPPL-1484 October 1978

*Exxon Nuclear Company

†Westinghouse Electric Corporation

Invited paper presented at IAEA Workshop on Neutral Injectors, Culham, England, June, 1978.

PLT NEUTRAL INJECTOR PERFORMANCE

L. R. Grisham, H. P. Eubank, H. F. Dylla, R. J. Goldston,
G. Schilling, L. D. Stewart*, R. W. Stookesberry†, M. Ulrickson
Plasma Physics Laboratory, Princeton University
Princeton, New Jersey 08540

ABSTRACT

The experience with respect to beamline operation on PLT and on the Princeton test stand is reviewed. We discuss the performance of the injectors, beam energy distributions as measured by two techniques, beam-associated impurities, control of gas evolution in the drift duct by titanium evaporation, reionization in the drift duct, and the computer archiving and control system currently under development.

---

*Exxon Nuclear Company.

†Westinghouse Electric Corporation.

INTRODUCTION

The neutral injection experiment on the Princeton Large Torus (PLT) has been underway for over a year now. The injection system employs four ORNL cusp-duopigatron sources on four beam lines designed and built at ORNL. This paper will review the experience thus far with respect to beam line operation on PLT and on the Princeton test stand. In particular, we will briefly discuss injector performance, beam species composition, impurities, titanium evaporation in the drift duct, reionization in the drift duct, and the evolving computer archiving and control system.

PERFORMANCE

The first beamline, using an ORNL 40 kV, 60 A source with grids drilled with holes out to a diameter of 20 cm, was installed on PLT last summer and began injection at modest power levels in September, 1977. It has since been run at levels as high as 41 kV and 62 A and has run reliably over considerable periods at 38-40 kV and 55-60 A. Injected neutral power when synchronized with a PLT plasma shot, as measured on a calorimeter inserted into the torus, has approached 650 kW using a hydrogen beam. Employing deuterium with its greater neutralization efficiency, we have injected as much as 800 kW into a PLT plasma. The arc efficiency on this source has typically been 900-1100 watts of arc power per amp of extracted beam current. In October, the second beam line, equipped with an ORNL 40 kV 70 A source carrying 22 cm grids, was brought into operation. It has since been run as high as 40 kV and 63 A, with routine operation at 38-40 kV and 55-60 A and typical injected hydrogen beam powers of 500 kW. Recently, the final two beamlines, one equipped with 20 cm grids and one with 22 cm grids, have been added to PLT. In general, the latter three sources have not exhibited quite as good arc efficiencies as did the first one. The second requires about 1100-1300 watts per amp of extracted current, while the latter

two typically require about 1100-1400 watts. The majority of the pulses which we have fired have been 100 msec long, although there have been a few pulses as long as 300 msec. Figure 1 shows a schematic of a PLT beamline, along with the interfacing to the computer control system under development.

BEAM SPECIES

The energy distribution in a neutral beam is a crucial factor since it has a strong influence on the beam penetration length and the resulting radial heating profile in the plasma. Moreover, wall and limiter sputtering is influenced by the beam species mixture since a larger percentage of fractional energy beam particles results in higher plasma edge temperatures, with the attendant more energetic charge exchange neutrals lost from the plasma.

The beam energy distribution can be determined through calorimetric techniques by magnetically deflecting the unneutralized ions on the beamline. While convenient, such techniques do not admit of determinations of any time dependence. Moreover, since the beam energy distribution is both significant and often controversial, the capability of measuring it by more than one method is highly desirable. We have used two alternative techniques to measure the energy distribution in beams at PPPL.

The first technique — measuring the relative intensities of the Doppler shifted and unshifted peaks of the H_α light from the beam — is a variation of the technique pioneered at LBL for use on TFTR beams.[1] Their technique employs an optical multichannel analyzer (OMA) and has direct optical access to the neutralizer cell. The system used here has a rapid scanning spectrometer instead of an OMA, which reduces the complexity of data acquisition since only one output signal is involved. A slight disadvantage of the scanning spectrometer approach is that the amplitude of the peaks corresponding to different beam species are obtained several msec apart, with the consequence that, if

they were present, variations in the source plasma species composition on a very short time scale could confuse the results. Inasmuch as there is no optical access to the neutralizer cell on this system, the beam must be viewed at the entrance to the drift tube, with the sight line intersecting the centerline of the beam at an angle of 18.5°. The lower gas pressure in the region near the drift duct results in a significant reduction in the light intensity, rendering Doppler broadening divergence methods impractical. The scanning system permits the completion of a scan in 20 msec. The particle distribution, representing the fraction of the beam particles at each energy, is obtained from the relative light intensities, and from the measured and calculated cross sections for H_α production. The distribution of beam power as a function of energy is easily obtained from the particle distribution.

This technique has thus far been employed on the Princeton PLT test stand, which is similar to a PLT beamline and is equipped with an ORNL 20 cm source similar to the first source in use on PLT. Figure 2 shows typical H_α intensity scans during neutral beam pulses at various accel voltages and currents. In each picture the spectrometer scans up, then down, with the right hand side thereby corresponding to conditions a few msec later in the beam pulse. The top four scans were all taken during the first half of 100 msec pulses. The bottom scan was taken during the latter half. No time dependence has been found in the beam energy composition, even when pulses 300 msec long have been used; consequently, the time required for a sweep poses no problems.

Table 1 shows the results obtained for the particle and energy fractions. The particle fractions shown correspond to neutral particles in the beam; thus, the atomic percentage in the source would be slightly higher than the indicated full energy percentage. The correction factor compensates for the differences in excitation cross sections at different energies and for the varying times

($\sqrt{E}$) spent in the observation region at differing energies. Generally, the results indicate that about 80-90% of the power is in the full energy component of the beam, while about 5-10% resides in each of the other two components.

The other technique used to measure the beam energy distribution involves firing a neutral beam into the PLT vacuum vessel at a hydrogen base pressure of about 4×10^{-6} T, with the toroidal and vertical fields energized. Beam neutrals entering the torus are stripped to ions by impact with the ambient hydrogen molecules. The resulting ions circumnavigate the torus along field lines, with their curvature B drift balanced by the chosen vertical field. The ions are subsequently lost by charge exchange with the H_2 molecules. Escaping the torus as neutrals, they are measured by the tangential electrostatic energy analyzer normally used for slowing down measurements.

A number of requirements must be satisfied in order to make good relative measurements of the abundances of the different species. First, we require that the integrated ionization probability ($n\sigma L$) along the path of the beam be small for all three energy components, so that the ionization profile in the torus is the same for each species, and the number of ionized particles is linearly related to the (known) stripping cross section. For the PLT geometry, this mandates that the pressure be less than 2×10^{-5} Torr (H_2).

Secondly, we assume that the ions are lost by charge exchange, and for simplicity we would like this loss to be toroidally invariant. To minimize the effect of loss due to the component of the curvature $\vec{B}$ drift which is not perfectly balanced out by the vertical field, we would like the ions to execute fewer than 10 transits of the torus. Conversely, to ensure toroidal symmetry, we would like the ions to circulate around the torus a few times before being lost. Defining an acceptable loss probability to be 0.25, we arrive at an optimum pressure of 4×10^{-6} Torr (H_2). The relative influx of particles at

each energy is then simply related to the raw signal at the neutral particle detector.

$$\text{Particle Flux (E)} \propto \frac{\text{Raw signal (E)}}{[\sigma_{01}(E)] \times \eta(E)}$$

where $\sigma_{01}(E)$ is the stripping cross-section for the injected H° atoms in the background H_2^0 gas of PLT, and $\eta(E)$ is the efficiency of the detector's helium-filled stripping cell at converting incoming neutrals into ions. At energies above about 5 keV, $\eta(E)$ is calculable from published cross sections for H° atoms and H^+ ions traversing He gas.

The experimental results, labeled "PLT C-X," are displayed at the bottom of Table 1. It is apparent that they are in good agreement with the spectroscopic measurements done on the test stand with a different source. We can see that not only is the species mix relatively insensitive to the extracted current (and consequently to the arc voltage and current); it also appears to vary little between sources. The results of Table I appear also to be in good agreement with calorimetric measurements made at ORNL by magnetic deflection of the unneutralized portion of the beam.

IMPURITIES

Another factor of great importance with respect to neutral injection is the chemical purity of the beam. It is well known that impurities, particularly ones of high atomic number, radiate prodigiously in Tokamak plasmas, with consequent cooling. Unfortunately, few measurements have been made of the contaminants accompanying neutral beams.

A prelimianry study has been made of the impurities accompanying the beam of the Princeton PLT test stand. Clean samples of beryllium and silicon were exposed to the beam in the target tank. Due to the constraints imposed by

the defining plates and drift duct, the beam was about 25 cm across at this point, with the samples being located 2.5 cm each side of the centerline. The silicon samples were shattered by the beam, but the beryllium survived. After exposure, the samples were analyzed by scanning Auger microscopy and ion backscatter techniques. Absolute impurity concentrations were determined using Rutherford backscattering of 2 MeV helium ions. (Courtesy of J. A. Borders and S. T. Picraux of Sandia Laboratories) The beryllium used was about 1.5 mm thick, and since the penetration range of both the incident and backscattered helium ions was much greater than the penetration range of the beam-deposited impurities, the determination was straightforward. Figure 3 shows a spectrum of the backscattered helium ions. The large peak corresponding to beryllium is just a consequence of the substrate. The genesis of the carbon and oxygen is uncertain; their presence may be partially due to the beam, but being ubiquitous in nature, they could also be the result of contamination by some other means (the sample was transferred in air). In this regard, we note that the spectroscopic energy analyzer on the test stand always shows a small peak just to the side of the unshifted light peak which is believed to correspond to either OH or H_2O accelerated in the beam. The aluminum peak is present because this was the material used for the sample holder. The scattering of small peaks above the aluminum peak is in the general mass range of sulfur and chlorine, both of which are common in stainless steel and could have come from the beamline. Moreover, the filaments are cleaned with hydrocloric acid. The very massive contaminant, which is tungsten and/or tantalum, almost certainly originates in the source since the oxide filaments use tantalum wires, and the emitting surface of the cathode plasma is stabilized by radially placed tungsten wires. The copper could originate from a number of sites: the plasma chamber, the grids, the neutralizer, or even the defining plates or the magnet face plates.

The iron could arise either from the drift duct or the second anode of the source. Table 2 summarizes the test stand results on impurity levels. The first column represents a sample exposed to only one beam pulse, the second column to a sample subjected to 50 shots. It is notable that less of each metal is observed on the 50 shot sample than the 1-shot sample, indicating that significant sputtering of the deposited impurities must occur with subsequent beam exposures. Thus, only the 1-shot sample impurity concentrations are used to calculate beam impurity levels. Because significant sputtering effects may also occur during the 100 ms single shot beam exposures, these values must also be considered a lower limit. We are planning exposures as a function of pulse duration to attempt to quantify possible sputtering effects. The third column of Table 2 shows that copper was observed on a silicon wafer exposed in PLT to 52 one-megawatt injection shots. This wafer was located at a random position in the torus (i.e., not directly across from a beam). The estimate of the beam impurity content from the PLT sample measurement assumes: (1) that the deposition is uniform over the PLT surface area ($\sim 2.5 \times 10^5$ cm^2); (2) that the deposition is not eroded by subsequent discharges and thus the deposition per discharge is linear with the number of discharges; and (3) the number of impurity atoms scales linearly with the beam pulse length and beam power. If one assumes that the observed Cu is an intrinsic beam impurity, then the estimated total amount of Cu (per beam line, per 100 ms pulse) roughly agrees for both the PLT and test stand measurements. No tungsten (or tantalum) were observed on the PLT sample, but 4×10^{15} represents the detection limit. Moreover, no iron was found on the PLT sample (1×10^{14} was the detection limit).

The PLT sources differ from the test stand source in that their second anodes are copper, rather than steel; hence it appears that the iron in the test stand beam originated primarily in the source, and not in sputtering off the drift duct walls. A final point

is that the test stand data were taken with an H° beam, while the PLT data were for D° beams. The fact that the copper level in PLT appears no higher than on the test stand even though D° is more efficient at sputtering than H°, suggests that the copper might be originating in the plasma chamber, where processes such as arcing and evaporation can play a role, rather than farther downstream. This would be consistent with the probable origin of the iron. Due to the uncertainties involved, however, this identification is at best tentative.

On PLT no significant difference has been noted in plasma impurity levels associated with injection by different beamlines. Whichever beamlines are injecting in the direction of the plasma current give rise to the lowest levels of plasma impurities, and the ones injecting counter to the current result in higher impurity levels. Reversing the direction of the plasma current results in a reversal of which beamlines give rise to higher impurity levels. Since the transmission efficiencies (percentage of power incident on beamline calorimeter which reaches PLT) on different lines range from 50% to 70%, this is further evidence that sputtering in the drift duct is probably not a major source of impurities in the plasma.

TITANIUM EVAPORATION IN THE DRIFT DUCT

The pressure in the drift duct of the Princeton PLT test stand has been measured during beam pulses in two different modes of operation. Initially, the walls of the drift duct were 304 L stainless steel with copper sputtered from the calorimeter plates covering about half of the area of the drift duct. Subsequently, about 20% of the drift duct walls were coated with titanium in an effort to reduce the pressure rise during beam pulses.

The pressure measurements were made using a Veeco RG-75 gauge located at the end of a 46 × 1.27 cm tube with a 90° bend located on the side of the calorimeter section about 1/3 of the distance from the main beamline box to the target

tank. In the second mode of operation a titanium getter ball was placed in the drift tube cryopump. Due to the ball's location only the walls of the drift tube pump box and the ends of the calorimeter plates which protude into the box were covered with titanium. The getter ball was run at an evaporation rate of 0.5 gm/hr for a period of one hour twice during the gettering experiment.

Figure 4(a) shows the pressure (corrected for the gauge sensitivity to H_2) as a function of pulse length with and without gettering and in the presence and absence of accel voltage. Figure 4(b) shows the corresponding pressure in the main beam line tank, with t=0 the time at which the accel voltage is turned on. Figure 5(a) shows the logarithm of the pressure in the drift tube with an arc pulse (but no accel voltage) with no titanium gettering, and Fig. 5(b) shows the same thing except with titanium gettering. Figures 6(a) and 6(b) show the same data after the getter was used. In the case of gettering and no accel there were not sufficient data to determine the slow time constant part of the pressure fall.

The pressure equilibration time for the drift tube should be about 8 msec. With a volume of 0.25 l and a conduction to the duct of 1.98 l/sec, the ion gauges' response time should be about 125 msec. Consequently, the time constant seen in the early part of the pressure fall is the time response of the gauge. However, the difference in the time behavior following a pulse between the accel and no accel cases shows some indication of outgassing caused by wall heating. The no accel time constants are the same within errors for the gettered and ungettered modes. The titanium may exert some pumping action just after the beam pulse as shown by the time constant for the accel-on data for the two modes, but the gauge response is not fast enough to be certain of this. The conductance of the duct is large compared to the pumping speed on the target chamber, with the result that the gas in the target chamber should be

pumped back through the duct with a time constant of about 650 msec, which is similar to the long time constant in the pressure fall data. The pressure difference between the cases with and without accel for a given mode (with or without gettering) is probably due in part to out-gassing of the target plate in the target tank.

Given the pressures and conductances, the gas evolution rate and total gas produced by the beam pulse can be determined. With no accel the only source of gas is that streaming from the source. The pressure gradient between the beam line tank, the drift tube, and the target tank indicates that this is about 1.5 torr-l/sec. This number is essentially the same in the gettered and ungettered modes. With no gettering the additional gas, because of the beam, varies from 1.0 torr-l/sec at 100 msec to 3.9 torr-l/sec at 300 msec. The rate of change of the gas production is 17.5 torr-l/sec^2 without titanium and 14.4 torr-l/sec^2 with the titanium. The pressure curves were unchanged by either repetition rate or number of pulses, indicating that the source of gas is not depleted during operation. Since the vapor pressure of H_2 at 4.2°K (the temperature of the cryopanels) is 6.0×10^{-6} torr, the titanium was almost being saturated with hydrogen as it was being deposited. This implies that the reduction of the rate of pressure rise must be due to a reduction of the evolution of gas from the titanium coated walls, rather than to any significant pumping action by the titanium. Thus, the titanium acts as a pacifier. We note that the reduction in the slope of the pressure rise was 20%, and the area covered by titanium was about 20% of the duct. The effect of the titanium was unchanged after two days of operation during which no additional titanium was deposited.

Integrating the pressure curves yields the total amount of gas produced. With no titanium there is 1.0 torr-l evolved during a 300 msec pulse; with

titanium the figure is 0.8 torr-l. These values exclude gas streaming from the source, representing instead additional gas evolved by the beam striking surfaces. Under the operating conditions during which these data were taken, about 250 KW of beam is lost in the drift duct; consequently about 1.65 torr-l/sec are being lost in this region. Such a deposition rate integrated over the pulse can account for only about 0.5 torr-l of gas. The remainder, 0.5 torr-l ungettered and 0.3 torr-l gettered, must be generated. Between 1/3 and 1/2 of this can be accounted for by outgassing of the calorimeter in the target tank, but the remaining amount must be evolved from the drift duct walls. Deposition of gas at a constant rate is not adequate to explain the pressure behavior since the rate of change of pressure at the end of the pulse requires a gas evolution rate of 3-4 torr-l/sec. If the power lost were uniformly distributed over the drift tube, the surface temperature rise would be only 5°C at the end of a 300 msec pulse. It is difficult to see how such a small change in the temperature could significantly affect the gas release rate. Of course, the power loss is probably not uniform, so hot spots may arise.

The principal conclusion from this experiment is that titanium gettering does reduce the pressure rise in the drift duct. Moreover, this reduction appears to be primarily due to a surface pacifying effect rather than to pumping.

REIONIZATION LOSSES IN THE DRIFT DUCT

During development of the PLT neutral beam injectors at ORNL an unexpectedly high pressure was observed in the drift duct during the beam pulse. Such a pressure rise poses a problem, since it increases the probability of beam neutrals being reionized in transit, with resulting losses to the duct walls in the presence of tokamak stray magnetic fields.

An analysis of Riviere and Sheffield,[2] later modified by Hemsworth,[3] had predicted the possibility of high duct pressure with resulting reionization

losses. Based on direct knock-off of gas from the wall by beam particles, their model predicts achievement of pressure equilibrium with a time constant similar to the duct pump-out time, typically ~ 10^{-3} sec.

In contrast, the pressure in the duct, the geometry of which is shown in Figure 7(a), of the PLT beam systems has been observed to increase linearly with time for at least 500 msec.[4] Moreover, the slope of the pressure rise has been found to vary linearly with beam power on the Princeton test stand, which, in conjunction with the first observation, implies that the pressure rise is linear with total energy — at least over the observed intervals. The time constant of this apparent linearity is longer than any system time constants except thermal ones, leading to the assumption that the pressure increase arises from thermal outgassing of the duct walls by stray beam power. Combining pressure rise data from ORNL and the Princeton test stand with the conductance and estimated power hitting the duct walls yields a factor, hereinafter referred to as the gas evolution coefficient C, of roughly 0.1 torr-l/sec/kJ for the observed pressure rise. The value of C appears to be independent of the beam pulse repetition rate and the number of preceeding pulses.

As anticipated, beam power attenuation in the presence of magnetic fields has been observed during PLT operation. Figure 7(b) shows power, normalized to extracted beam power and equilibrium neutral fraction, transmitted to the PLT calorimeter inside the torus as a function of perveance. This is a compilation of all data on the PLT east (#1) beamline, for 100 msec H° pulses in the high-impedence mode (in which most of the gas is fed into the expansion chamber). These conditions were chosen for analysis because they were the best documented. Figure 7(b) reveals a marked decrease in the transmitted power in the presence of PLT fields. An increase in losses with greater integrated beam energy is indicated in Fig. 8(a), showing transmitted power (normalized to optimum perveance) as a function of total ion beam energy (IVt) times

the equilibrium neutral fraction, f_0^∞, which product should be proportional to power through the duct. Points accompanied by error bars represent at least 10 observations, while the two without error bars are single observations. If the pressure rises observed on the test stands are used to predict the reionization losses, the predictions run less than those in Fig. 8(a), and this discrepancy increases with $IVtf_0^\infty$. The discrepancy can be resolved by considering an additional pressure rise due to additional wall heating and outgassing by the reionized power.

To model the pressure rise we assume losses in the drift duct to be due to beam attenuation:

$$P = P_0 \exp(-\sigma n l)$$

where P_0 is the power which would have reached the plasma in the absence of reionization losses, σ is the ionization cross section, and nl is the duct line density. The line density, calculated self-consistently as due in part to the reionized power, is given by:

$$nl = n_0 l + n_\theta l + n_r l \quad ,$$

where $n_0 l$ is the line density in the absence of duct heating, $n_0 l$ is the line density due to direct interception of the beam power by the duct walls, and $n_r l$ is the line density due to wall heating by the reionized power. In the calculations, it is assumed that

$$nl = (n_0 + n_\theta + n_r)l$$

where l is the duct length and n_0 is the density without duct heating. The density arising from wall heating by directly intercepted power, n_θ, is given by

$$n_\theta = \frac{C}{F} \varepsilon P_0 t$$

where C is the gas evolution coefficient, F is the pumping speed for gas in the duct, ϵ is the fraction of power which is directly intercepted by the duct walls, and t is the time the beam has been on. The density due to wall heating by the reionized power, n_r, is given by:

$$n_r = \frac{C}{F}(P_o - P)t \quad .$$

Traditionally design work and injected power predictions have used the above model with $n_\theta = n_r = 0$.

Figure 8(b) shows the data of Fig. 8(a) (with the no-field data replaced by a line at the average) along with the predictions of the model, using the PLT data. To simulate calorimeter data the predicted power has been time-averaged. It is apparent that the value C = 0.1 torr-l/sec/kJ inferred from the test stand is compatible with the data, although a somewhat lower or higher ($\pm$ .05) value of the coefficient could also lie within the errors, particularly as the two points most strongly determining the slope represent single measurements. It is worth noting in this regard that, since 1/3 to 1/2 of the pressure rise on the test stand may have been due to pumping of the target tank gas, the inferred gas evolution coefficient could be too high by a similar amount.

Figure 9(a) displays data on the increase in the PLT plasma density during injection as a function of injected neutral power. Also shown is the predicted density rise with a 450 kW, 35 keV neutral beam if the density increase were due to ionization of beam neutrals only, and the predicted rise due to ionization of beam neutrals plus half the neutrals evolved in the duct according to the model (the remaining half being assumed to go to the beam cryopump). It appears that the model predicts a gas flux which correlates with the plasma density increase appreciably better than the beam-only prediction.

Figure 9(b) gives the predicted neutral power to PLT as a function of the time the beam has been on. The lowest curve reflects the high impedance arc condition under which the first beamline was initially operated. Also shown are curves indicating the predicted power with decreased outgassing (due to titanium coating of the duct) and with the optics obtained by the addition of precel voltage at ORNL.

As mentioned above, the data base for this model consisted entirely of pulses with the source running in the high impedance mode. The low impedance mode is obtained by increasing the gas feed to the cathode plasma region, while decreasing the gas to the expansion chamber somewhat, thus resulting in lower arc voltages. Subsequent operation in this mode on the PLT East (#1) beamline (the one used for the model data) appears to have resulted in a significant reduction in reionization losses. This mode is less well documented than the high impedance mode, but it appears that there is usually very little ($\lesssim$ 3%) reduction in transmitted power when comparing shots with and without the PLT fields at 500 kW for 100 msec. This amelioration is attributed to better source optics in the low impedance mode. There is still some accumulation of gas in the duct however, and transmission might deteriorate at much longer pulse lengths. Figure 10 shows a comparison between accel current traces for the two modes and between the light generated in the duct for the two modes. It is apparent that, although the light generated at 100 msec is lower in the low impedance mode, the slope is nearly the same as that of the high impedance mode, even though the current for the low impedance mode is decreasing. Hence, while the low impedance mode significantly proves transmission, it is by no means a complete solution.

Recently the PLT East beamline has been run on D° with 800 kW of transmitted power for 150 msec with no significant drop ($\lesssim$ 2%) between shots with and without PLT fields.

Examination of the equations for reionization losses and duct pressure rise, along with a small argument expansion of the exponential, leads to a trouble parameter, ltP_0/F, by which neutral beam systems can be classified with respect to potential reionization loss problems. In the trouble parameter l is the duct length, t is the pulse length, P_0 is the desired transmitted power, and F is the conductance for evolved gas escaping the duct. The larger the parameter, the greater the potential for problems. The values of the parameter in joules-sec/cm^2 for some beam line designs are: 2.7 for PLT, 0.7 for the present Doublet III, 0.8 for the present PDX, and 4.8 for TFTR.

NEUTRAL BEAMLINE MONITORING AND CONTROL

A PDP 11/10 processor system has been used for both monitoring and control of the Princeton test stand beam, and, more recently, of one of the PLT beamlines. Automatic control of the accel modulator tube voltage has been achieved in the range between 15 kV and 30 kV, with the arc voltage, rectifier voltage, and bending magnet current tracking to maintain near optimum source conditions. A total of about 12 shots are required to span the above 15 kV range in a well conditioned source. A PDP 11/34 is currently being implemented for dedicated monitoring and eventual control of the four PLT beamlines.

FUTURE PROGRAM

Aside from neutral injection into PLT, PDX, and TFTR, future plans at Princeton Plasma Physics Laboratory include looking more closely at beam associated impurities with an E × B analyzer and studying the drift duct pressure rise and possible mechanisms to account for and to control it. In particular, the effects of titanium gettering on some of the PLT beam lines will be explored.

ACKNOWLEDGMENT

This work was supported by the U.S. Department of Energy under contract number EY-76-C-02-3073.

REFERENCES

(1) C. F. Burrel, W. S. Cooper, and W. F. Steele, Spectroscopic Diagnostics for Neutral Beam Injectors, 1977 IEEE Conference, Troy, N. Y.

(2) A. C. Riviere and J. Sheffiend, Nuc. Fus. 15 (1975) 944.

(3) R. S. Hemsworth, Culham Laboratory Report CLM-R162 (1976).

(4) W. K. Dagenhart, et al., ORNL/TM-6374 (1978), Oak Ridge National Laboratory.

TABLE I.

DOPPLER SHIFTED H_α RESULTS

Voltage	Species	Raw Data	Correction	Particle Fraction	Power Fraction
20 kV	H_1	1.0	1.0	0.64 ± 0.04	0.83 ± 0.02
	H_2	0.44 ± 0.11	0.326	0.09 ± 0.03	0.06 ± 0.02
	H_3	1.92 ± 0.37	0.217	0.27 ± 0.05	0.12 ± 0.03
25 kV	H_1	1.0	1.0	0.73 ± 0.02	0.87 ± 0.02
	H_2	0.54 ± 0.09	0.297	0.12 ± 0.02	0.07 ± 0.02
	H_3	1.18 ± 0.14	0.181	0.15 ± 0.01	0.06 ± 0.01
30 kV	H_1	1.0	1.0	0.71 ± 0.03	0.85 ± 0.02
	H_2	0.74 ± 0.16	0.269	0.14 ± 0.03	0.09 ± 0.02
	H_3	1.25 ± 0.16	0.157	0.14 ± 0.02	0.06 ± 0.01
35 kV	H_1	1.0	1.0	0.76 ± 0.03	0.88 ± 0.02
	H_2	0.70 ± 0.18	0.226	0.12 ± 0.03	0.07 ± 0.02
	H_3	1.12 ± 0.15	0.130	0.11 ± 0.02	0.04 ± 0.01
PLT C-X	H_1		1.0	0.74 ± 0.04	0.87 ± 0.03
	H_2		0.27 ± 0.10	0.14 ± 0.04	0.09 ± 0.03
	H_3		0.14 ± 0.04	0.12 ± 0.03	0.04 ± 0.01

TABLE II.

	1 H° Shot at 30 kV 40 A on Test Stand (100 ms pulse)			50 H° Shots at 30 kV 40 A on Test Stand (100 ms pulse)	52 High Power Shots - 1 MW D° Injection on PLT		
	Fe	Cu	W or Ta	Fe	Cu	Fe	W or Ta
Impurity (cm^{-2}) Concentration	2.9×10^{14}	3.2×10^{14}	1.3×10^{13}	0.9×10^{14}	4×10^{14}	$<1 \times 10^{14}$	$<5 \times 10^{12}$
Impurity Fraction in Beam (%)	1.2	1.3	0.5	—	—	—	—
Total Impurity in Beam	2.1×10^{17}	2.3×10^{17}	9.0×10^{15}	—	4.8×10^{17}	$<1.2 \times 10^{17}$	$<6 \times 10^{15}$
Impurity Fraction in PLT at $\bar{n} = 2 \times 10^{13}$/cc	0.26	0.29	0.01	—	.16	<.15	0.008

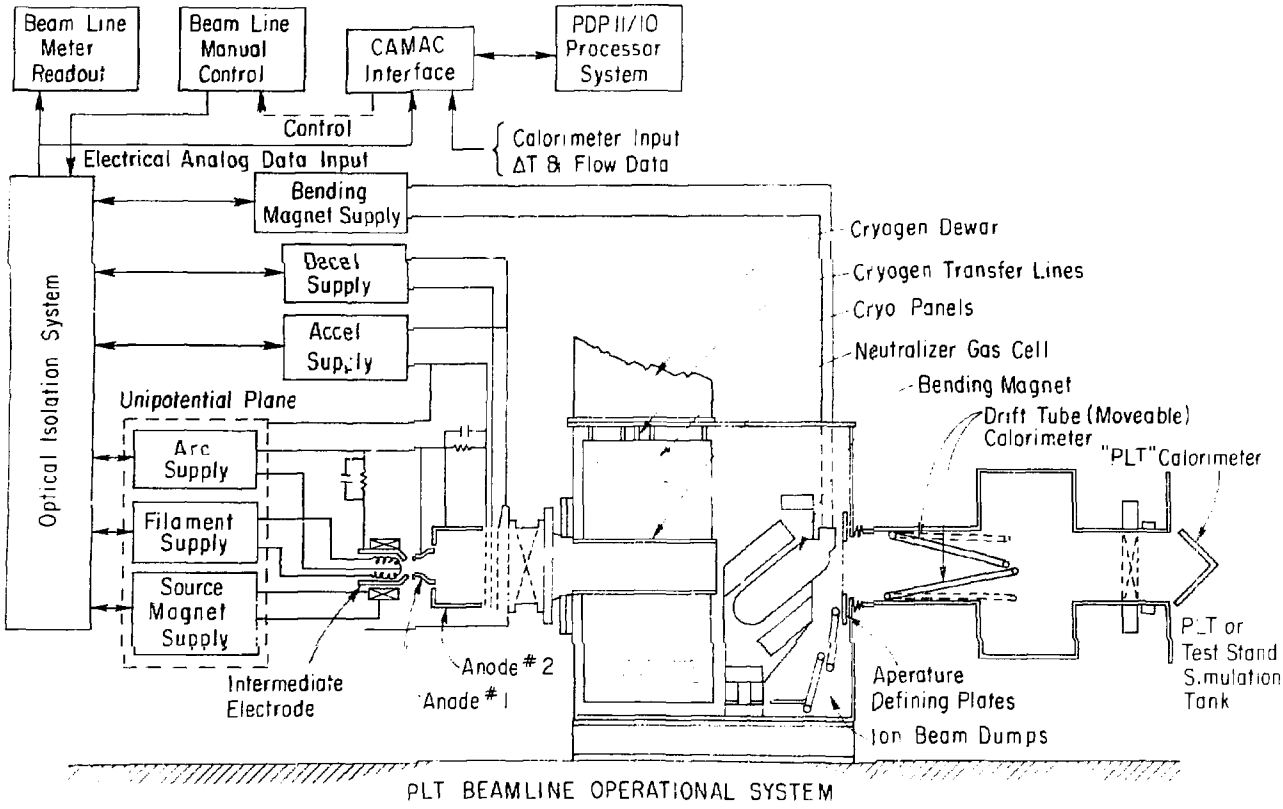

Figure 1. Diagram of a PLT beamline, shown with provisions for computer monitoring and control which are under development. #783563

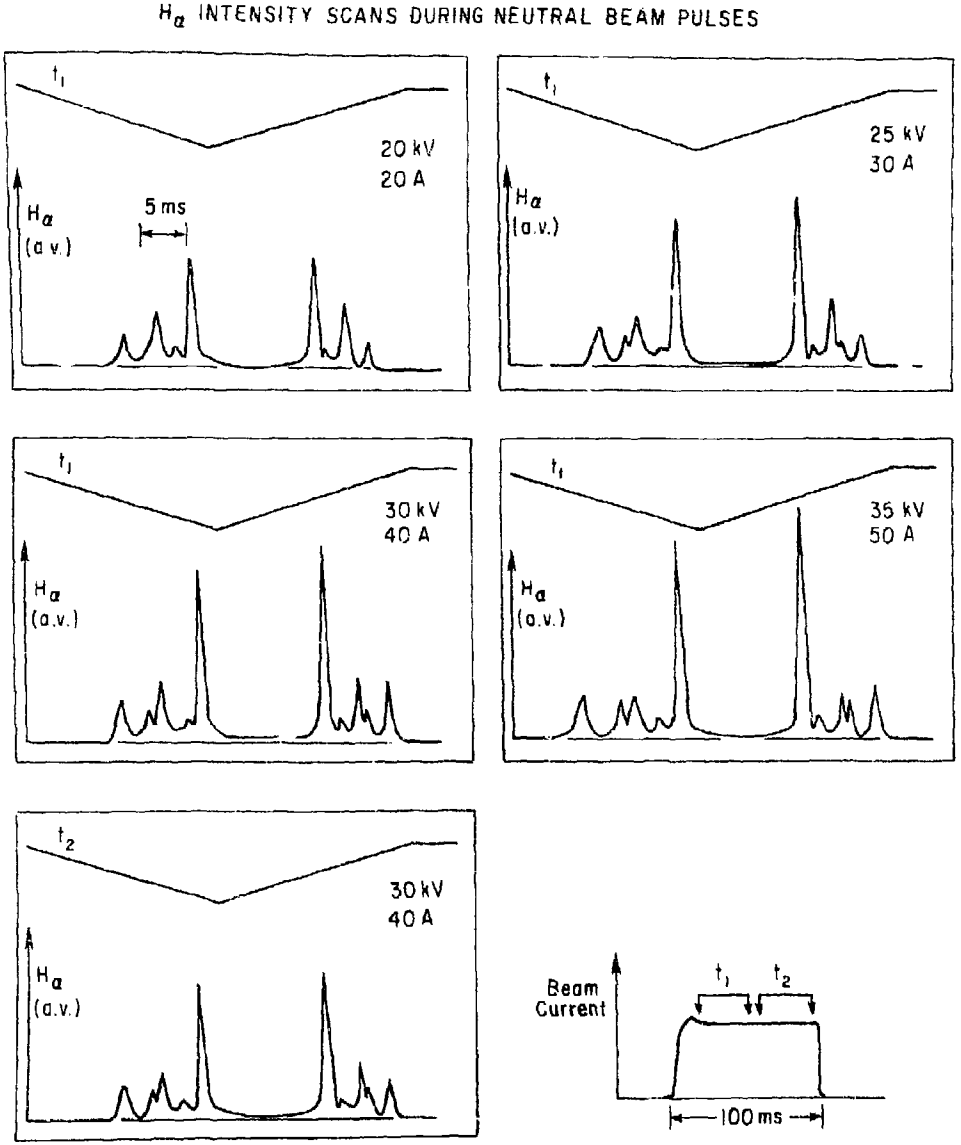

Figure 2. H_α intensity scans during neutral beam pulses.
#783480

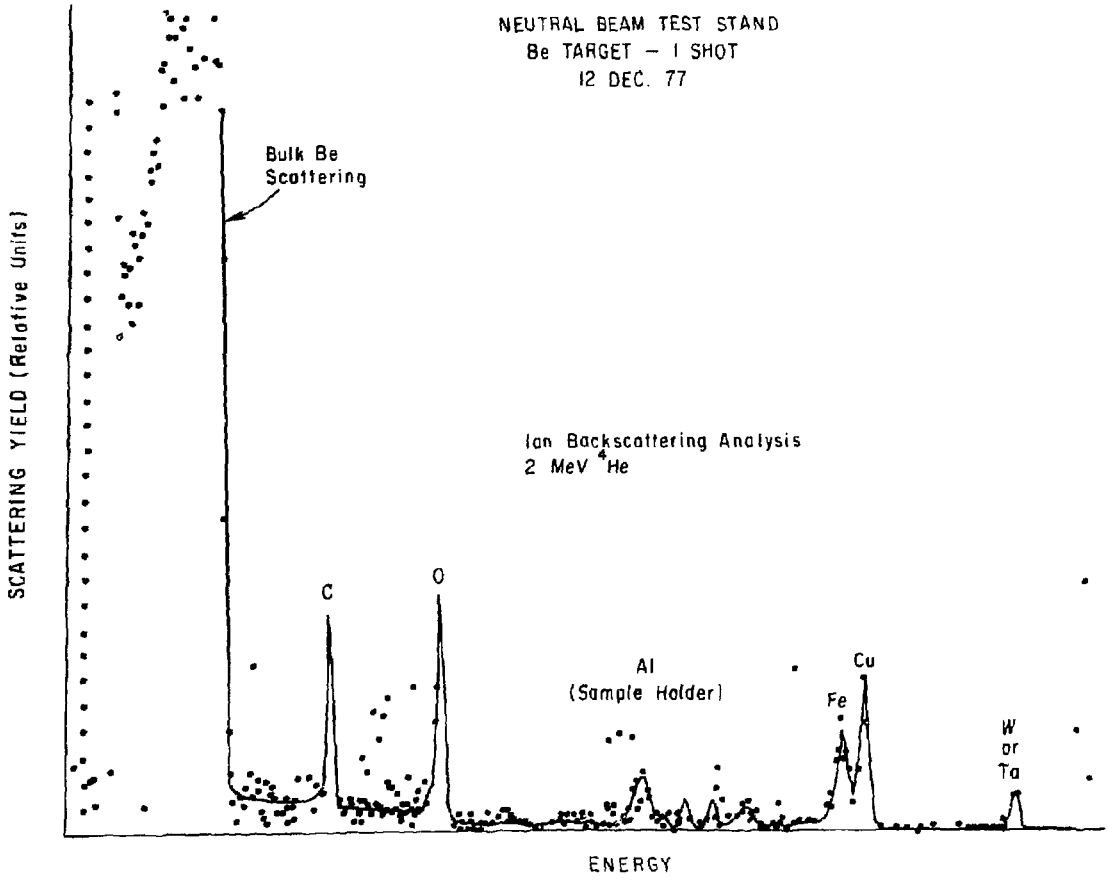

Figure 3. He^4 2.0 MeV backscattering spectrum from beryllium sample exposed to neutral beam. #783717

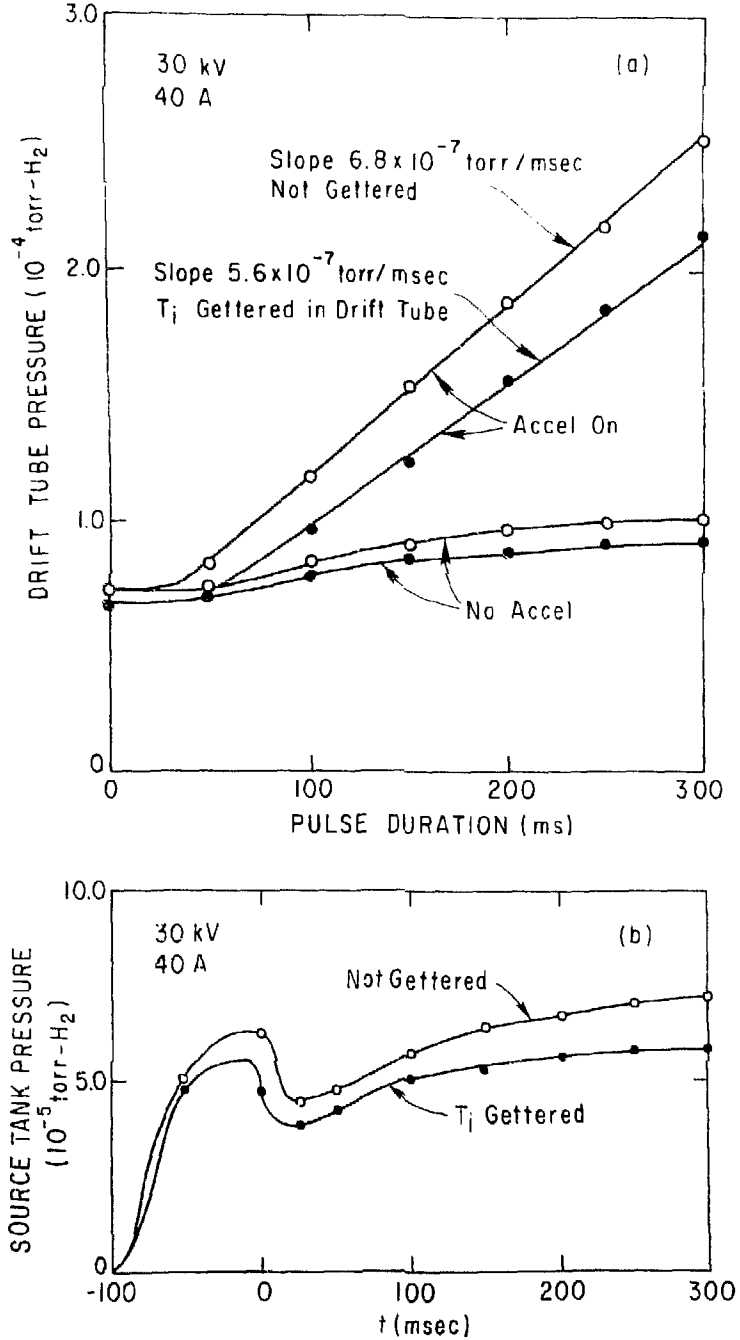

Figure 4. (a) Pressure in the drift duct as a function of pulse length.
(b) Pressure in the source tank during a beam pulse. #783723

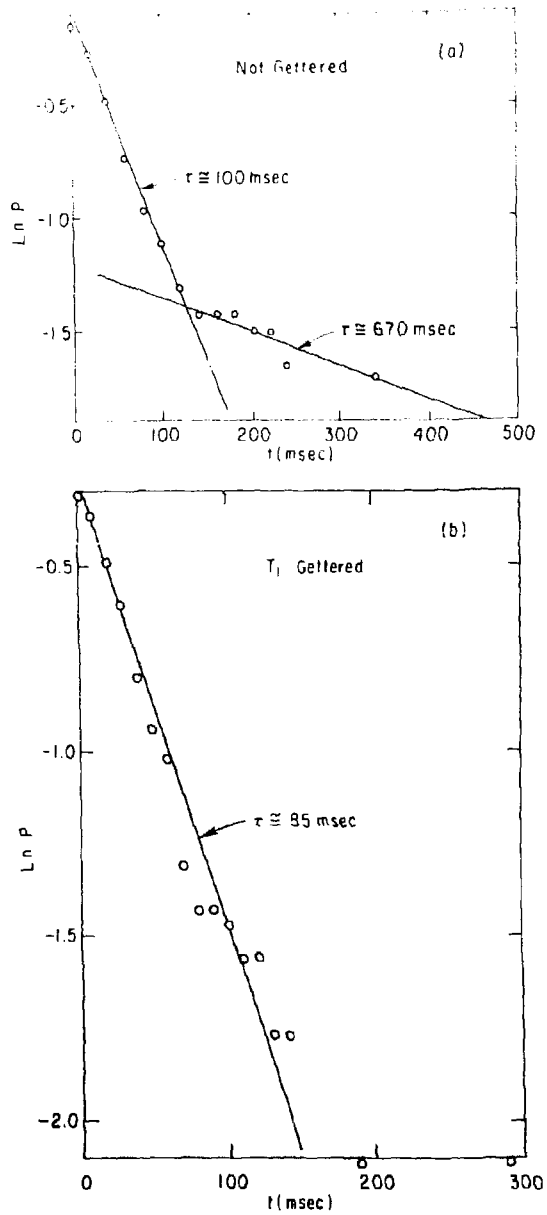

Figure 5. (a) Pressure fall in the drift tube with no beam and no titanium gettering.
(b) Pressure fall in the drift tube with no beam and with titanium gettering.

#783722

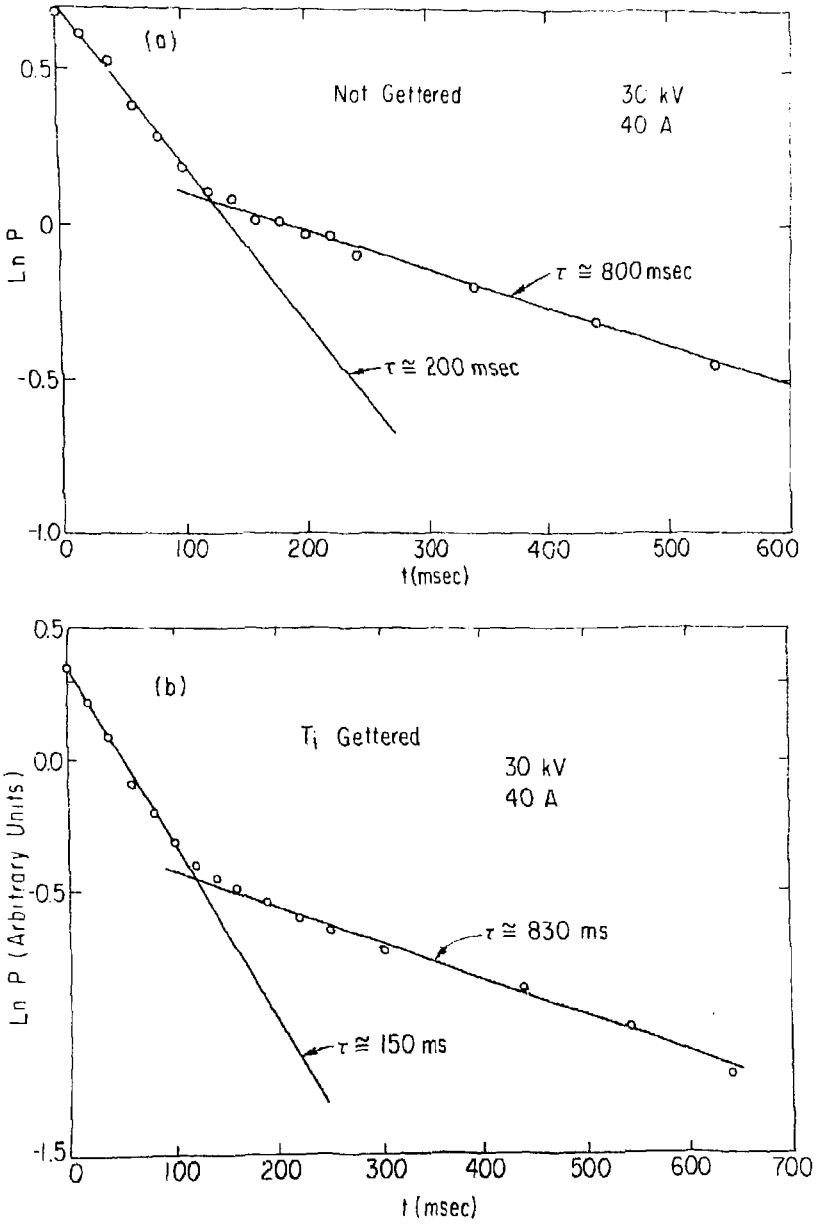

Figure 6. (a) Pressure fall in the drift tube with beam and no titanium gettering.
(b) Pressure fall in the drift tube with beam and with titanium gettering. #783721

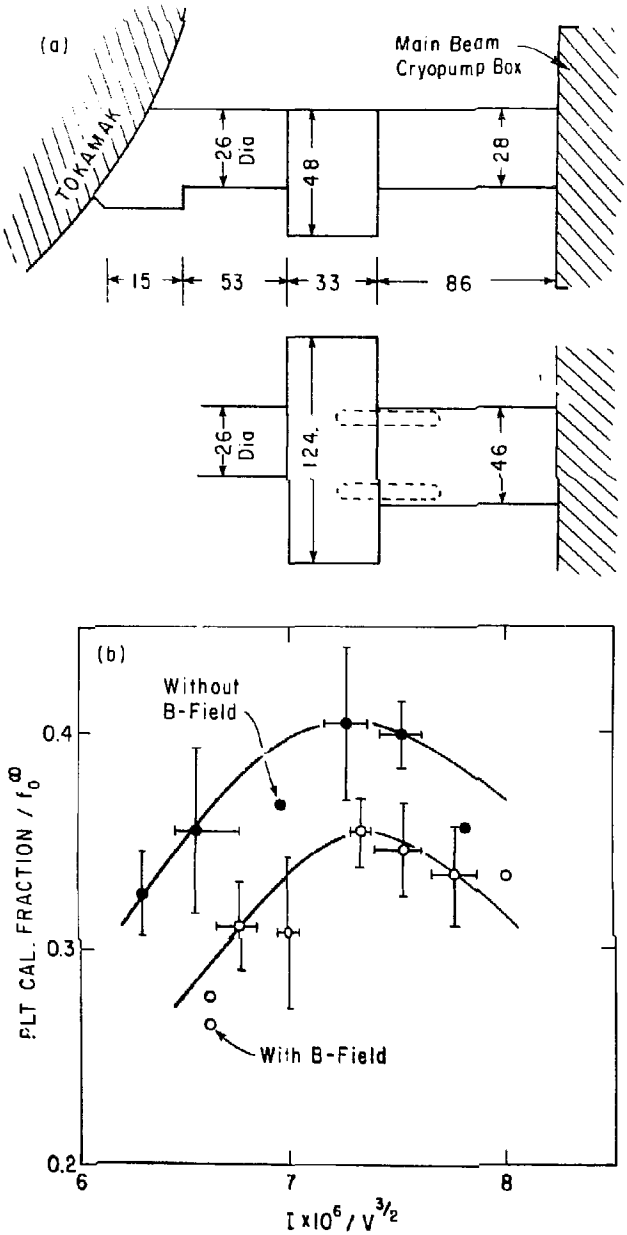

Figure 7. (a) PLT drift duct geometry (dimensions are in cm).
(b) PLT beam transmission as a function of perveance.
#783718

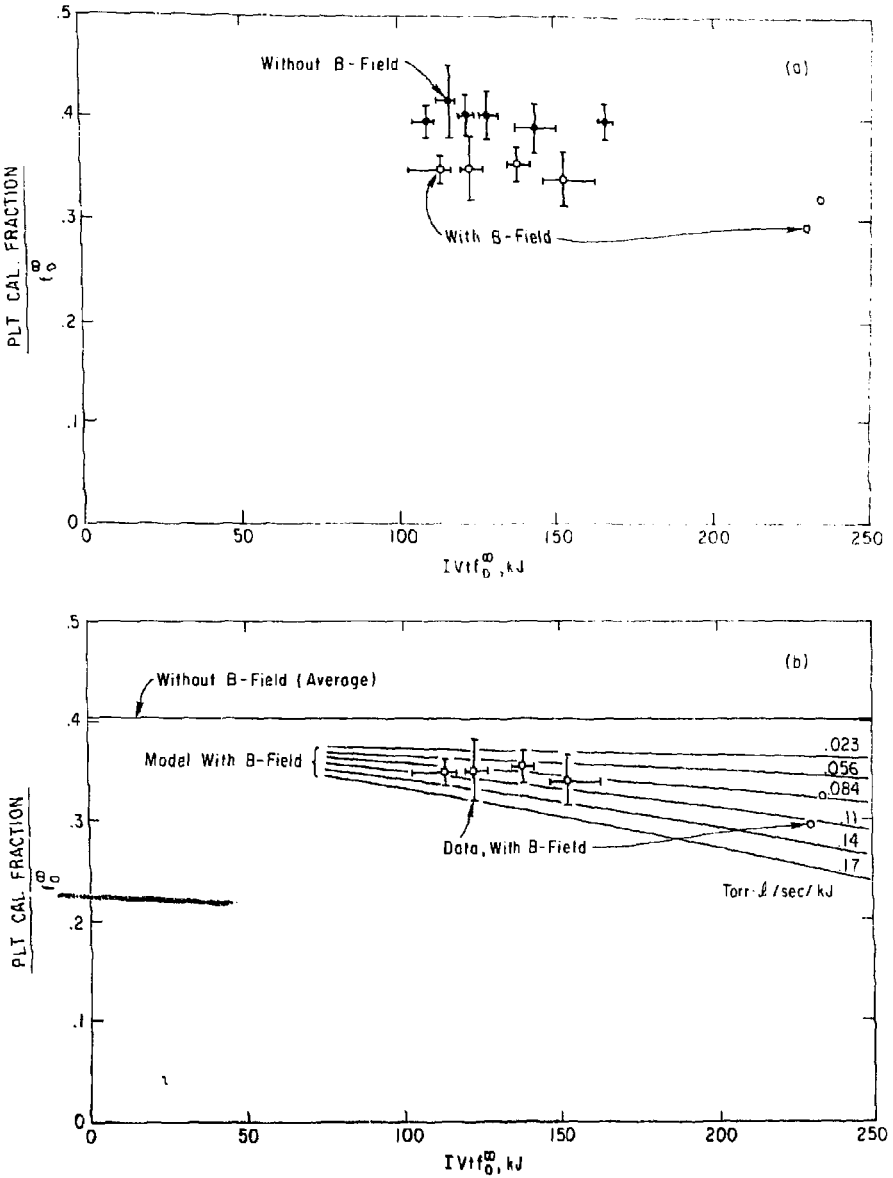

Figure 8. (a) PLT beam transmission as a function of $IVtf_0^\infty$.
(b) Measured PLT beam transmission compared with transmission predicted by reionization loss model. #783720

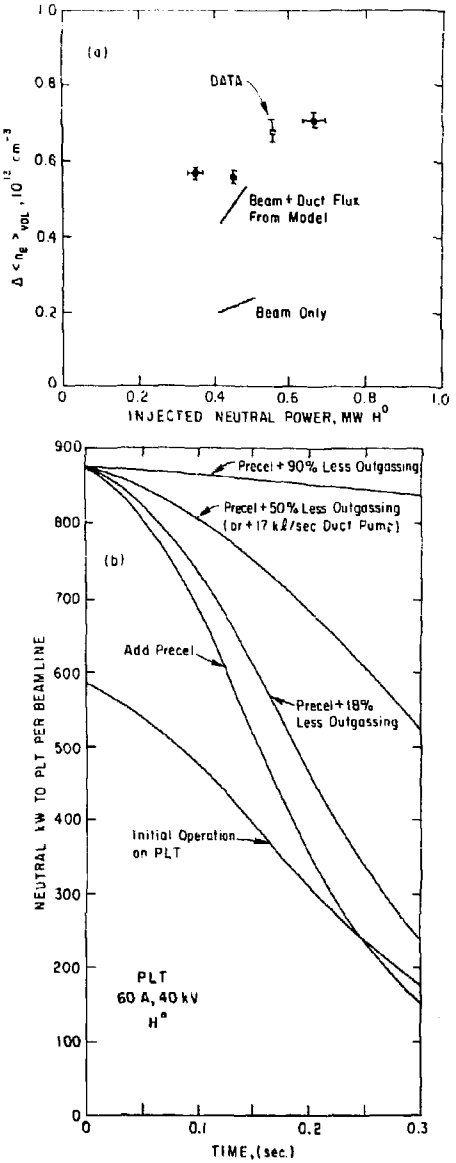

Figure 9. (a) Measured and predicted PLT plasma electron density increase as a function of injected neutral beam power.
(b) Predicted PLT injected neutral power. #783719

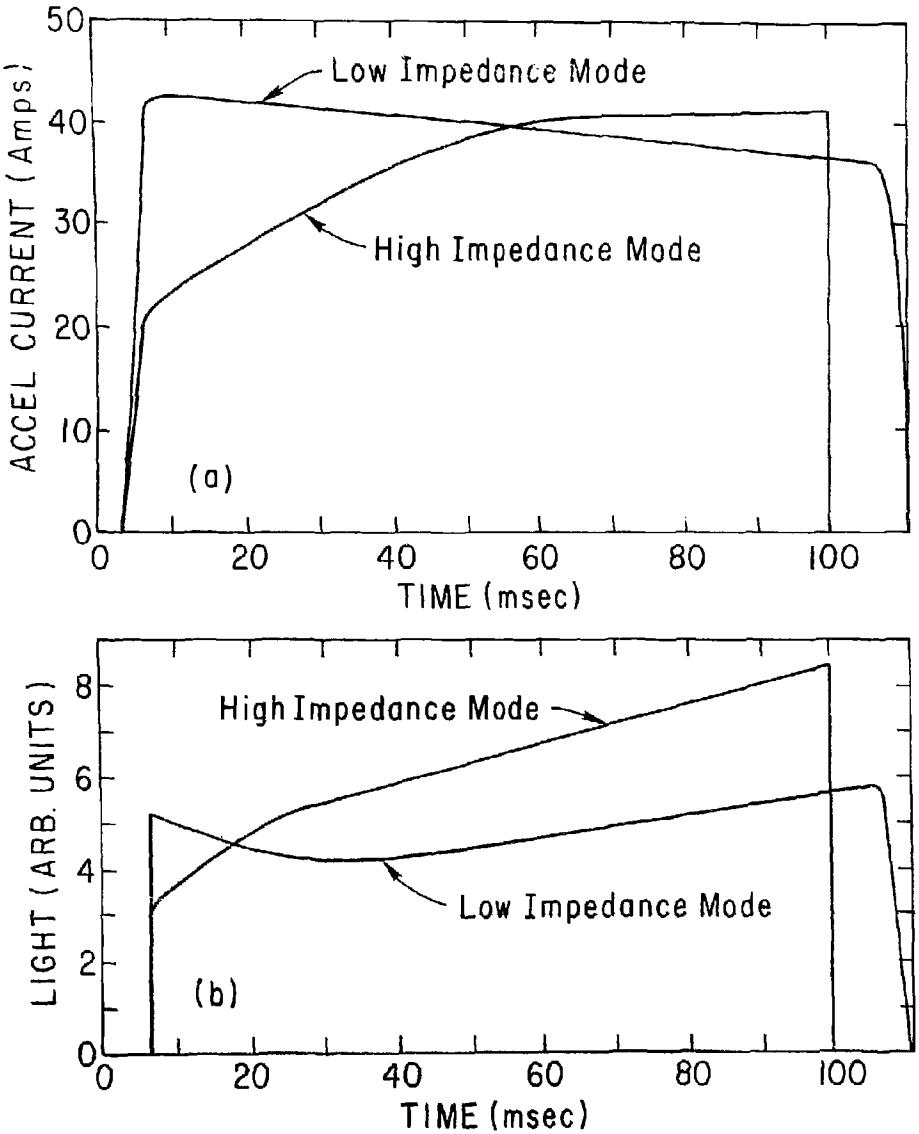

Figure 10. Accel current and duct light emission for the high impedance and low impedance modes of source operation. #783737